How to cite: *Angew. Chem. Int. Ed.* **2023,** *62,* e202218316
International Edition: doi.org/10.1002/anie.202218316
German Edition: doi.org/10.1002/ange.202218316

Solid-State Batteries

Evaluation and Improvement of the Stability of Poly(ethylene oxide)-based Solid-state Batteries with High-Voltage Cathodes

Yuriy Yusim, Enrico Trevisanello, Raffael Ruess, Felix H. Richter, Alexander Mayer, Dominic Bresser, Stefano Passerini, Jürgen Janek, and Anja Henss**

Abstract: Solid-state batteries (SSBs) with high-voltage cathode active materials (CAMs) such as $LiNi_{1-x-y}Co_xMn_yO_2$ (NCM) and poly(ethylene oxide) (PEO) suffer from "noisy voltage" related cell failure. Moreover, reports on their long-term cycling performance with high-voltage CAMs are not consistent. In this work, we verified that the penetration of lithium dendrites through the solid polymer electrolyte (SPE) indeed causes such "noisy voltage cell failure". This problem can be overcome by a simple modification of the SPE using higher molecular weight PEO, resulting in an improved cycling stability compared to lower molecular weight PEO. Furthermore, X-ray photoelectron spectroscopy analysis confirms the formation of oxidative degradation products after cycling with NCM, for what Fourier transform infrared spectroscopy is not suitable as an analytical technique due to its limited surface sensitivity. Overall, our results help to critically evaluate and improve the stability of PEO-based SSBs.

Introduction

State-of-the-art lithium-ion batteries (LIBs) are expected to soon reach their physicochemical limits in terms of energy density.[1] Solid-state batteries (SSBs) are currently one of the most promising concepts to surpass the limitations of LIBs and could be another step towards a society that is less dependent on fossil fuels.[1–3] By replacing flammable liquid electrolytes in LIBs with solid electrolytes (SEs), not only safety is expected to be improved, but also higher energy densities might be achieved by introducing a lithium metal anode.[1,4] A large variety of SEs are currently under intensive investigation. Polymer-,[5] oxide-,[6] halide-[7] and thiophosphate-based[8] SEs show satisfactory properties with different material-specific advantages and disadvantages for practical applications. Among all SEs, solid polymer electrolytes (SPEs) based on poly(ethylene oxide) (PEO) and lithium bis(trifluoromethanesulfonyl)imide (LiTFSI) as conducting salt have been successfully commercialized by Blue Solutions (Bolloré Group) and are currently utilized by Daimler in the electric bus "eCitaro" with $LiFePO_4$ (LFP) as cathode active material (CAM).[9] The practical use of PEO-based SPEs is particularly attractive because they have numerous advantages, including low cost and high flexibility, thereby allowing good interfacial contact to the electrode active materials, the capability of solvating lithium salts and moderate ionic conductivity at elevated temperatures ($\approx 1\,mS\,cm^{-1}$ at 80 °C).[10–14] Despite these characteristics, PEO-based SSBs still face several challenges on the way to large-scale high-energy density applications. Substituting LFP with high-voltage CAMs, such as $LiCoO_2$ (LCO) and nickel-rich $LiNi_{1-x-y}Co_xMn_yO_2$ (NCM) or $LiNi_{1-x-y}Co_xAl_yO_2$ (NCA), would allow a significant increase in energy density.[15–17] In this context, the oxidative stability of the SPE has often been questioned and investigated in the literature. The findings are very contradictory, with the oxidation onset of the SPE being reported to be 3.2 V,[18] 4.0 V[19,20] or even 4.6 V vs. Li^+/Li.[21] As recently discussed by Hernández et al.,[22] the different values of the oxidation onset are highly dependent on the electrochemical measurement methodology. In addition, PEO-based SSBs in combination with high-voltage cathodes experience sudden cell failure related to "voltage noise" during charging. This has often been attributed to oxidation processes of the PEO-based SPE at the cathode.[23] In contrast, in their recent work, Homann et al.[21,24] attributed this cell failure to the formation of lithium dendrites at the anode. Increasing the thickness of the SPE membrane resulted in "voltage noise-free" operation, suggesting that indeed dendrites are the origin of "voltage noise" and cell failure. Nevertheless, direct evidence for the formation of lithium dendrites has not yet been provided. Furthermore, the long-term cycling

[*] Y. Yusim, E. Trevisanello, Dr. R. Ruess, Dr. F. H. Richter, Prof. Dr. Dr. h.c. J. Janek, Dr. A. Henss
Institute of Physical Chemistry, Justus Liebig University Giessen
Heinrich-Buff-Ring 17, 35392 Giessen (Germany)
and
Center for Materials Research (ZfM/LaMa), Justus Liebig University Giessen
Heinrich-Buff-Ring 16, 35392 Giessen (Germany)
E-mail: juergen.janek@phys.chemie.uni-giessen.de
anja.henss@phys.chemie.uni-giessen.de
Dr. A. Mayer, Dr. D. Bresser, Prof. Dr. S. Passerini
Helmholtz Institute Ulm (HIU)
Helmholtzstraße 11, 89081 Ulm (Germany)
and
Karlsruhe Institute of Technology (KIT)
P.O. Box 3640, 76021 Karlsruhe (Germany)

performance with high-voltage cathodes such as LCO in PEO-based cells without cell failure also varies strongly in the literature. While data from Qiu et al. show a discharge capacity of less than 10 mAh g^{-1} after 5 cycles,[10] data from Wang et al. show a discharge capacity of over 100 mAh g^{-1} after 50 cycles.[25] Based on the contradictory results on cell failure and capacity decay of PEO-based SSBs published in the literature, we reinvestigated the compatibility and reactivity of PEO-LiTFSI with high-voltage cathode active materials, such as LCO and NCM. By separating the anode and cathode half cells with a LATP ($Li_{1.4}Al_{0.4}Ti_{1.6}(PO_4)_3$) ceramic solid electrolyte we unequivocally confirm that the "voltage noise" failure is indeed caused by dendrite formation at the anode and not by oxidative processes at the cathode. To overcome this limitation, we increased the mechanical rigidity of the SPE by using PEO with a higher molecular weight, which effectively eliminates the "voltage noise" related cell failure, enabling stable cycling operation. Moreover, we also confirm with XPS the formation of carbonyl groups as oxidative degradation products at the cathode/SPE interface, for what Fourier transform infrared spectroscopy is not suitable due to its limited surface sensitivity.

Results and Discussion

Due to the contradictory results and conclusions on PEO-based SSBs with high-voltage cathodes found in the literature, we first addressed the question of whether the noisy voltage is caused by dendrites or by oxidative processes at the cathode. Thereby, we investigated the origin of this behavior in comparison to the previous results in literature and propose a simple modification of the SPE in order to overcome the "voltage noise" failure, extending former work by Homann et al..[24] In the second part, we look at the stability of the composite cathode. We investigate the cathode side by demonstrating the influence of cell leakage on the cycling performance and SPE decomposition mechanisms.

Evaluation and elimination of "noisy voltage" related cell failure

A Li | PEO-LiTFSI | $LiNi_{0.83}Co_{0.11}Mn_{0.06}O_2$/PVDF/Super P cell was constructed using a PEO-based SPE with a molecular weight $M_w = 300\,000$ g mol^{-1} as separator and cycled between 3.0 V and 4.3 V against a lithium metal anode at 0.1 C (1 C = 200 mA g^{-1}) and 60 °C. The charge and discharge voltage profiles of the first cycle are shown in Figure 1. As demonstrated in Figure 1, the galvanostatic cycling of the PEO-based SSB shows a "voltage noise" behavior in the initial two charge curves, in good agreement with the report by Homann et al., who also observe such a behavior already at around 3.75 V[21,24] In this context, the authors suggested that the formation of lithium metal dendrites is responsible for this failure, since increasing the thickness of the SPE separator and/or replacing the lithium

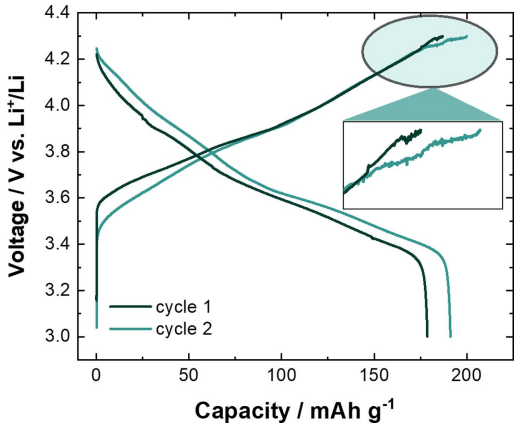

Figure 1. Galvanostatic cycling data of a Li | PEO-LiTFSI | $LiNi_{0.83}Co_{0.11}Mn_{0.06}O_2$/PVDF/Super P cell within a voltage range of 3.0–4.3 V vs. Li^+/Li at 0.1 C and 60 °C using PEO with $M_w = 300\,000$ g mol^{-1}. Charge and discharge curves of a cell. Magnified view of "voltage noise" behavior.

metal with a graphite anode eliminated this failure.[21] In contrast, this failure was attributed by Simonetti et al.[23] as a clear indication for oxidation processes of the PEO electrolyte. Besides, a possible corrosion of the aluminum current collector should be considered, since LiTFSI-containing electrolytes are known to corrode at high voltages (> 3.8 V vs. Li^+/Li) and lead to characteristic pitting.[26,27] To exclude the possibility that this process affects the "voltage noise" behavior and cycling stability of PEO-based SSBs with high voltage cathodes, the aluminum current collector was examined with SEM before and after electrochemical cycling (4 cycles with "voltage noise"). As shown in Figure S1, no difference in the morphology of the aluminum current collector can be seen. Hence, we exclude corrosion of Al-foil of LiTFSI containing SPE as a potential cause of the "voltage noise" behavior.

To evaluate, whether the oxidative degradation of PEO-based SPEs at the cathode or dendrite formation at the anode lead to observed "noisy voltage" cell failure, a LATP pellet was placed between the anode and cathode, as demonstrated in Figure 2a. In this case, the LATP pellet acts as a mechanically rigid separator that prevents the penetration of lithium dendrites through the SPE. Since the SPE is still in physical contact with the NCM cathode, the setup enables possible oxidative processes to occur at the NCM | SPE interface, but precludes lithium dendrite penetration. In addition, the LATP pellet acts as a "white screen" for lithium dendrites. In the case of Li dendrite penetration through the SPE, lithium metal hits the LATP on its way from the anode to the cathode, leading to an immediate reduction of Ti^{4+} to Ti^{3+} of LATP, which is a widely known problem at the interfaces of LATP with Li metal.[28,29] The presence of reduction products can be detected by color changes on the LATP pellet, which is white in its pristine state (Figure 2c).[30] In contrast to Gupta et al.,[31] who visualized the penetration of Li-dendrites in symmetric cells with operando SEM, our approach is much simpler and easier to adopt. Based on this idea, we constructed the Li | PEO-LiTFSI | LATP | PEO-LiTFSI | $LiNi_{0.83}Co_{0.11}Mn_{0.06}O_2$/

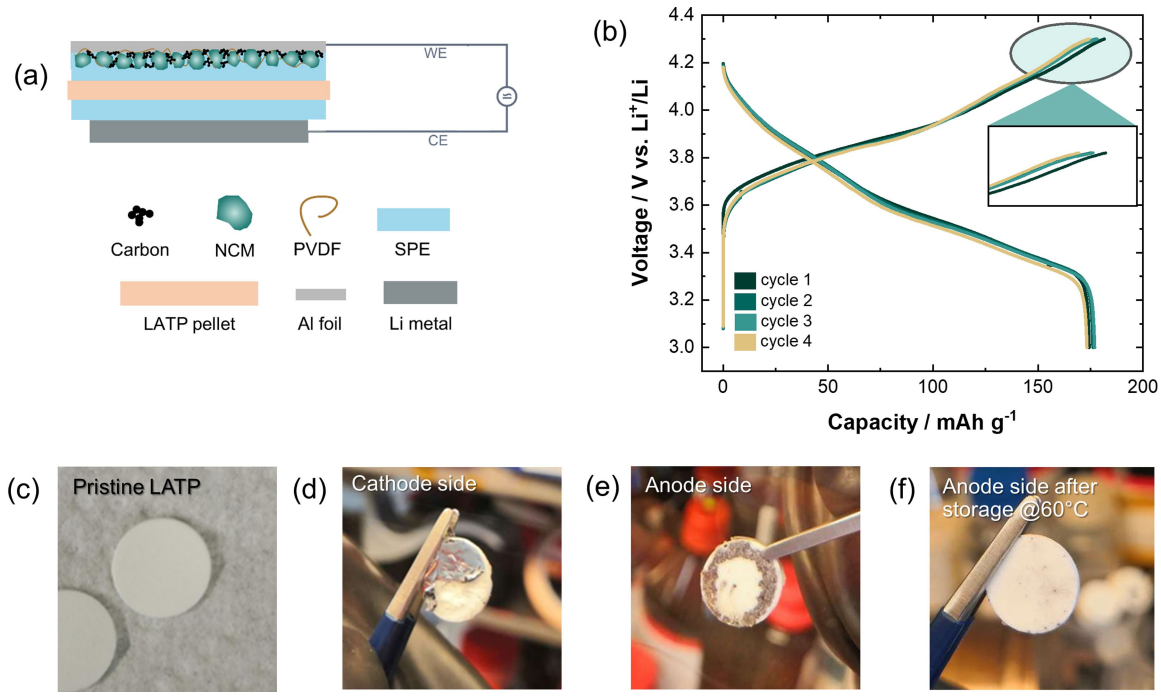

Figure 2. Results from experiments to verify potential dendrite penetration as cause for "voltage noise" failure. (a) Experimental Scheme of the Li | PEO-LiTFSI | LATP | PEO-LiTFSI | $LiNi_{0.83}Co_{0.11}Mn_{0.06}O_2$/PVDF/Super P cell using PEO with $M_w = 300\,000\ g\,mol^{-1}$. (b) Galvanostatic cycling data within a voltage range of 3.0–4.3 V vs. Li^+/Li at 0.1 C and 60 °C. (c) Pristine LATP-pellet. (d) LATP after electrochemical cycling after cathode and SPE removal (cathode side). (e) LATP after electrochemical cycling and after lithium and SPE removal (anode side). (f) LATP after storage at 60 °C without cell cycling and after lithium and SPE removal (anode side).

PVDF/Super P cell and cycled it between 3.0 and 4.3 V vs. Li^+/Li at 0.1 C and 60 °C for 4 cycles. The cycling data are shown in Figure 2b. It should be noted that the LATP pellet leads to an increase in cell impedance and, thus, to a high overpotential which eventually results in a lower initial capacity. Nevertheless, no "voltage noise" behavior was detected. This confirms that the "voltage noise" failure is obviously not a result of PEO oxidation, proving that the reason is definitely not located at the cathode side, but may be caused by the poor mechanical properties of the low molecular weight PEO that allows dendrites to penetrate through the SPE, as proposed by Homann et al.[21,24] To confirm this, after cell disassembly the anode, the cathode and the SPE from both sides were carefully removed. It should be noted that the separation of the sticky PEO based SPE membrane from the LATP is challenging (a common issue of post-mortem analysis of PEO-based solid state batteries[10,21]). As shown in Figure 2d, no color changes on the LATP on the cathode side were observed (the aluminum current collector with the cathode could not be completely removed). This indicates that no lithium dendrites have penetrated through the LATP. However, a grey colored ring of "flake"-like structures can be seen on the LATP pellet on the anode side in Figure 2e. This indicates that lithium dendrites penetrated into the SPE membrane and caused a reaction of the LATP that resulted in a color change. Interestingly, complete coverage of the reduction products on the LATP is not achieved, suggesting that the lithium dendrites mainly penetrate along the edges, which could be the path of least resistance/most external force and most detrimental shrinkage of the SPE when the viscosity of the SPE decreases due to the elevated temperature. In addition, no color changes of the SPE were observed after peeling off the SPE at the anode and cathode side. To exclude the possibility that this behavior is caused by direct contact between the anode and LATP due to shrinkage of the SPE at elevated temperature and applied pressure rather than dendrite formation and growth, we stored a cell at 60 °C at OCV (open-circuit voltage) for about 4 days. As described above, anode and the SPE were removed, obtaining a white LATP pellet without color changes (Figure 2f). This confirms unequivocally that indeed the penetration of dendrites through the SPE is the cause of the "voltage noise" cell failure. In addition, direct contact between the anode and cathode would result in a voltage drop to 0, which was not observed (see Figure 1). Overall, based on the observed color changes on the LATP due to the lithium dendrites, we conclude that lithium dendrites penetrate through the SPE membrane, causing the "voltage noise" behavior and eventually leading to cell failure, which is in good agreement with the results by Homann et al.[21]

To prevent lithium dendrite penetration in a more practical way than increasing the separator thickness[21] or using a spacer[32] and as an alternative to a crosslinked PEO-based SPE,[24] the mechanical strength of the SPE can also be increased by using PEO with a higher molecular weight (here: $M_w = 8\,000\,000\ g\,mol^{-1}$). This is in good agreement with investigations by Wang et al.,[33] who measured the

dependence of tensile strength on the molecular weight of PEO and reported higher tensile strength for higher molecular weights. We observed that at 60 °C PEO-LITFSI with $M_w = 300000\ g\,mol^{-1}$ seems to thermally deform, while PEO-LITFSI with $M_w = 8000000\ g\,mol^{-1}$ keeps its shape. The poor mechanical properties of low molecular weight PEO at 60 °C are shown in the report of Homann et al.[24] As reported by Devaux et al.,[34] the conductivity reaches a plateau above a molecular weight of $10^4\ g\,mol^{-1}$, which means that no significant conductivity losses are expected when further increasing M_w. Thus, a conductivity of about 1 mS cm^{-1} at 80 °C (see Figure S2) can be achieved with PEO-based SPEs with $M_w = 8000000\ g\,mol^{-1}$, which is sufficient to reach full initial cell discharge capacity (> 200 mAh g^{-1} for Ni-rich NCM) (Figure 3). Furthermore, PEO with higher molecular weight enables noise-free charge/discharge cycling in SSBs with NCM, as shown in Figure 3 (no LATP separator was used), in contrast to low molecular weight PEO. To support this, the experiment shown in Figure 2 was repeated, however, using PEO-based SPE with $M_w = 8000000\ g\,mol^{-1}$ at 80 °C. After disassembling the cell and removing PEO and lithium from the anode side, an intact LATP pellet without any color changes was obtained (see Figure 3). This confirms that PEO with higher molecular weight effectively suppresses the penetration of lithium dendrites through the SPE, whereas for lower molecular weight PEO, failure occurs in the first cycle (Figure 1).

In conclusion, we confirm that the "noisy voltage" failure is caused by lithium dendrite formation on the anode side due to the low mechanical strength of low molecular weight PEO-based SPEs rather than by PEO oxidation at the cathode. Indeed, lithium dendrite penetration can be considered as one cell failure mode, which can lead to serious safety concerns. In addition, we demonstrate that the use of PEO with a high molecular weight ($M_w = 8000000\ g\,mol^{-1}$) is a practical and simple way to prevent such cell failure and to enable long-term cyclability of high-voltage PEO-based SSBs compared to lower molecular weight PEO. To the best of our knowledge this modification of the SPE has not been presented so far to overcome the "noisy voltage" failure in PEO-based SSBs. Furthermore, this modification enables to achieve high initial discharge capacities (> 200 mAh g^{-1}) with Ni-rich NCM, which have not been achieved in previous studies.[21,24,32] The dependence of the "voltage noise" failure on the utilized CAM and applied voltage is part of future studies.

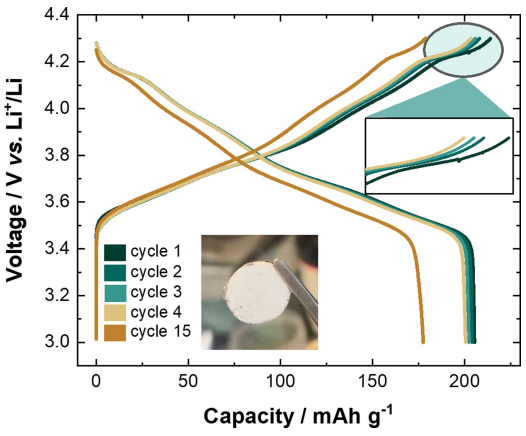

Figure 3. Galvanostatic cycling data of a Li | PEO-LiTFSI | $LiNi_{0.83}Co_{0.11}Mn_{0.06}O_2$/PVDF/Super P cell within a voltage range of 3.0–4.3 V vs. Li^+/Li at 0.1 C and 80 °C using PEO with $M_w = 8000000\ g\,mol^{-1}$. Magnified view without "voltage noise" behavior.

Evaluation of long-term stability and electrolyte oxidation

After evaluating and improving the anode side, we subsequently investigated the long-term cycling behavior of PEO-based SSBs considering the electrolyte oxidation with focus on the cathode side. For this purpose, Li | PEO-LiTFSI | $LiCoO_2$/PEO-LiTFSI/PVDF/Super P cells were prepared and cycled for 40 cycles between 3.0 V and 4.2 V vs. Li^+/Li at 0.1 C and 60 °C using the PEO-based SPE with a molecular weight of $M_w = 8000000\ g\,mol^{-1}$. The corresponding discharge capacities and Coulomb efficiency as a function of cycle number are shown in Figure 4a. As described above, the penetration of lithium dendrites leading to "voltage noise" behavior was effectively avoided by using the SPE with a higher molecular weight. The discharge capacity decreases from to 110 mAh g^{-1} to 97 mAh g^{-1} after 40 cycles (capacity retention of 89 %). This

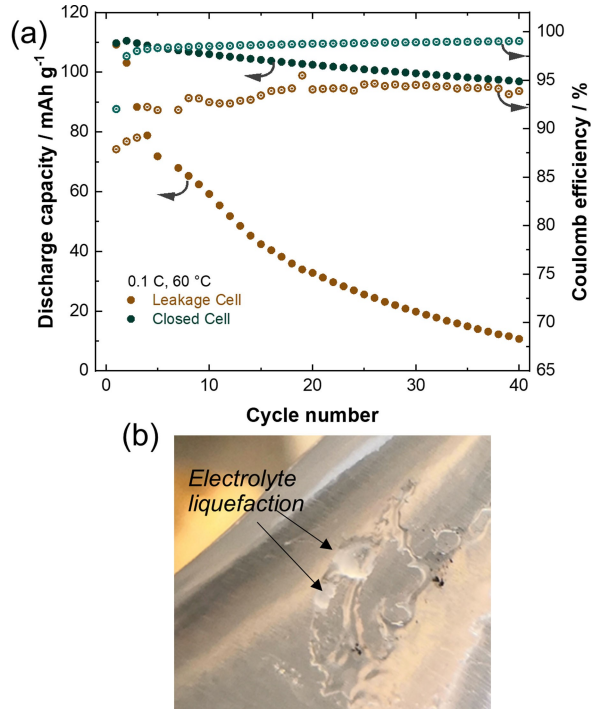

Figure 4. (a) Discharge capacity and Coulomb efficiency as function cycle number of "closed" and "leakage" Li | PEO-LiTFSI | $LiCoO_2$/PEO-LiTFSI/PVDF/Super P cells within a voltage range of 3.0–4.2 V vs. Li^+/Li at 0.1 C and 60 °C using PEO with $M_w = 8000000\ g\,mol^{-1}$. (b) Residues of liquefied electrolyte on the pouch bag walls obtained from cells with leakage after electrochemical cycling.

capacity fading is in good agreement with the data presented by Wang et al.[25] using similar cycling parameters. In contrast, the data of Qiu et al.[10] show a discharge capacity of less than 5 mAh g^{-1} after 10 cycles (capacity retention of 5 %), which is significantly different from the data demonstrated in this study and by Wang et al..[25] One reason for this large difference in capacity fading can be failures in the experimental setup, which can be easily overlooked. We have found that, for example, unexpected leakage in the cell during cell operation significantly affects electrochemical cycle performance. So, we built cells that were intentionally not properly sealed leading to constant exposure to air and moisture during cell operation. In the following, the properly closed cell is denoted as "closed cell" and the other with intentional leakage as "leakage cell". In Figure 4a, the discharge capacity of the leakage cell after 40 cycles is 11.3 mAh g^{-1} (capacity retention of 10 %), which is significantly worse than that of the closed cell. Of course, this is to be expected, since the lithium metal anode is sensitive to air and moisture.[35] Interestingly, the cycle performance of the leakage cell correspond well to the data by Qiu et al.[10] Hence, the reason for the significant differences in cycle performance cannot be fully clarified. However, these results highlight that easily overlooked inaccuracies in the experimental setup can affect the cycling performance and lead to misinterpretation of data. In addition, after disassembling the leakage cells after cycling of PEO with M_w = 8 000 000 g mol^{-1} in air, we found a liquid-like polymer film inside the pouch bag as shown in Figure 4b. These liquid-like polymer residues were never obtained in closed cells after cycling. Thus, we assume a swelling process of the SPE due to moisture in the atmosphere. Interestingly, such liquid phase has already been observed in literature by Nie et al.[20] reporting the presence of liquid residues after cycling to high voltages, but not relating this to potential cell leakage.

However, because Nie et al. charged their cells to 4.6 V vs. Li$^+$/Li, which significantly extends the electrochemical stability window of LCO,[36,37] a direct comparison with our study is difficult (cells were only cycled to 4.2 V vs. Li$^+$/Li in our study). We examined the liquid-like polymer residues by nuclear magnetic resonance (NMR) spectroscopy. The spectrum obtained is shown in S3 and reveals degradation products that we attribute to the decomposition of SPE by caused by cell leakage and entrance of atmospheric gas. The degradation mechanism in cells with leakage is beyond the scope of this work, but is an interesting issue as the consequences for cell failure may be severe.

Overall, we suggest that the observation of liquid phases of the SPE may indicate cell leakage or residual moisture in the cell. We further note that SPE liquefaction due to leakage in the cell will further accelerate the short-circuit behavior and failure of the cell (c.f. above).

To investigate possible degradation of PEO-based SPEs in high-voltage cathode composites, post mortem Fourier transform infrared (FTIR) spectroscopy was carried out, which is commonly used in this context in literature.[38,10,18] We like to note that FTIR is not spatially resolving, so any information is averaged over the cathode composite. Spatially resolved information was additionally observed by XPS, see below. For the FTIR analysis, samples of the SPE were collected after electrochemical cycling. To ensure reliability and reproducibility of the data, three different spots were measured, obtaining consistent results. Special care was taken to examine electrolyte residues from the vicinity of the cathode/SPE interface, since oxidative processes are to be expected there according to literature.[38,18,10,16] In Figure 5a, FTIR spectra of the pristine PEO-based SPE and the SPE after 40 cycles with LCO are shown. The spectra agree very well, suggesting that no decomposition products were formed by electrochemical cycling of PEO-based SPEs with high-voltage cathodes we formed. In contrast, according to Qiu et al.[10] two additional peaks after electrochemical cycling would be expected in the spectral region between 1750 cm^{-1} and 1600 cm^{-1} which correspond to the C=O stretching mode assigned to the carbonyl functional groups of aldehyde, ketone or ester species, indicating oxidative decomposition processes of the SPE.[39] However, these oxidative decomposition products are absent in our study, as shown in Figure 5b. This is in good agreement with the observations of Seidl et al.[18] and Ma et al.,[38] who also did not report the presence of carbonyl groups after cycling the SPE with NCM or LCO. The latter one was cycled even to higher voltage (4.5 V vs. Li$^+$/Li). Interestingly, after analysis of the cells with leakage (see above) we indeed found these C=O functional groups, as presented in Figure 5b. This indicates that cell leakage can lead to undesirable oxidative decomposition reactions that can easily be mistakenly associated with high-voltage degradation. A formation mechanism for these oxidized species under the influence of moisture and air in the atmosphere is beyond the scope of this work. However, according to our FTIR data, they do not form in appropriately assembled and closed PEO-based cells after electrochemical cycling to higher voltages. Therefore, utmost care must be taken during preparation of cells to avoid any residual moisture or leakage that would cause such rapid degradation.

In addition, post-mortem FTIR analysis was performed with PEO-based SPE which was cycled with NCM for 25 cycles between 3.0–4.3 V vs. Li$^+$/Li at 60 °C and 0.1 C. Consistent with previous results, no C=O functional groups were obtained (see Figure S4). The FTIR spectra of the pristine PEO-based SPE and cycled SPE are presented in Figure 5c. Upon closer inspection, some changes in the entire FTIR spectrum were observed after electrochemical cycling, some of which are comparable to the results of Seidl et al.[18] and Ma et al..[38] According to Seidl et al.[18] and Ma et al.,[38] these changes were attributed to the decomposition of the SPE, in particular to chemical changes of the conducting salt.[38,18] In this context, we prepared an additional sample of the pristine SPE and measured a FTIR spectrum after heating to 70 °C, which is shown in red in Figure 5c. Interestingly, the FTIR spectrum of the pristine SPE after heating to 70 °C corresponds very well with the cycled sample. This suggests that mentioned position shifts and intensity differences are not caused by electrochemical cycling to higher voltage but by heat treatment. In the spectral range of 1200–1000 cm^{-1} the crystalline phase is

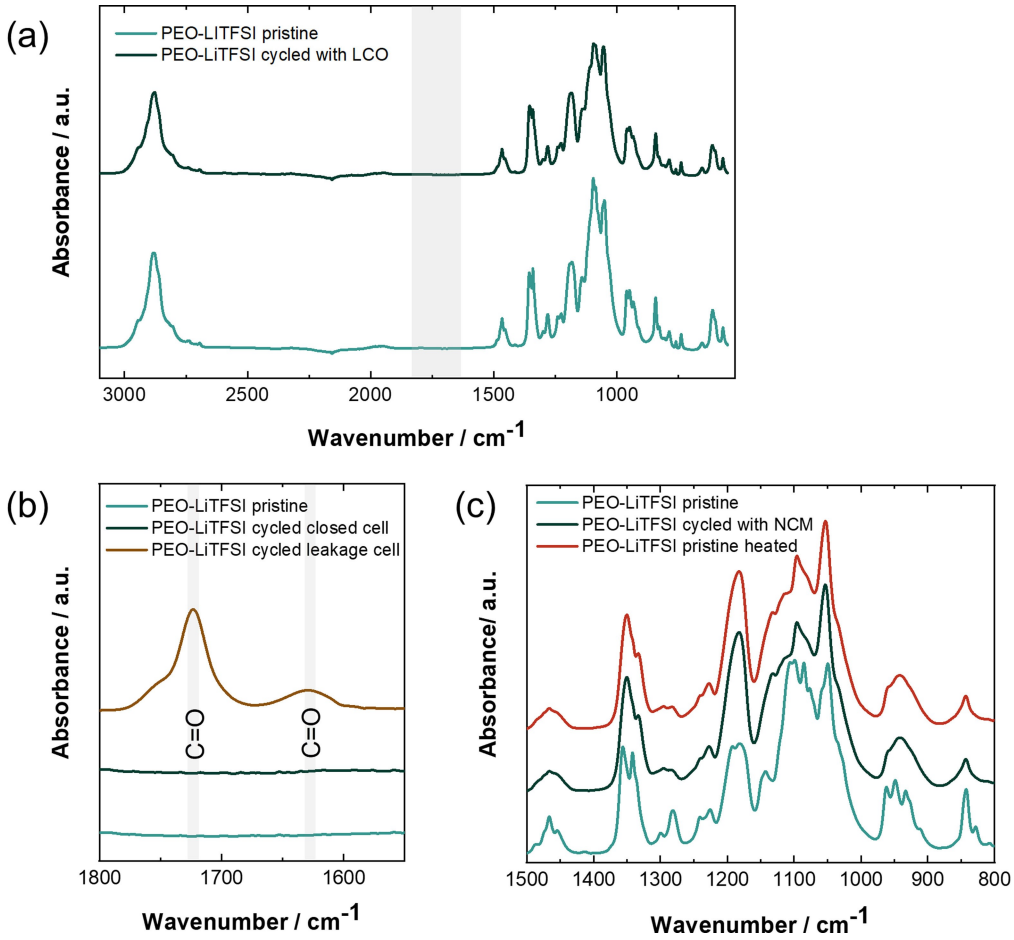

Figure 5. FTIR spectra of PEO-based SPE before and after electrochemical cycling. (a), (b) Cells were cycled with LCO within a voltage range of 3.0–4.2 V vs. Li^+/Li at 0.1 C and 60 °C for 40 cycles using PEO with $M_w = 8\,000\,000\ g\,mol^{-1}$. (c) Cells were cycled with NCM within a voltage range of 3.0–4.3 V vs. Li^+/Li at 0.1 C and 80 °C for 25 cycles using PEO with $M_w = 300\,000\ g\,mol^{-1}$. A spacer for stable cycling operation was used.

featured by the characteristic peaks at 1142, 1091 and 1053 cm^{-1} that mainly correspond to symmetric and asymmetric C–O–C stretching vibrational modes of PEO, which is well documented in literature.[40–42] If PEO is now heated to 70 °C, the fraction of crystalline phase is reduced and the amorphous fraction increases. Interestingly, the corresponding temperature-dependent spectra of pure PEO in the range between 1400 and 800 cm^{-1} as shown by Dissanayake et al.[43] are fully consistent with our SPE data before and after heating. Therefore, the observed changes in FTIR are not caused by any cycling-induced degradation of the PEO, but rather an effect of temperature. We further note that these changes were not seen in the FTIR spectrum in Figure 5a, since a SPE based on higher molecular weight was used, which has a higher tendency for crystallization (c.f. above).

Since FTIR is not a surface-sensitive technique[44] and only offers spatially average information, we also investigated the NCM/SPE interface with X-ray photoelectron spectroscopy (XPS) to identify possible decomposition products near the interface. Therefore, the PEO-based SSBs were assembled and charged to 4.1 V or 4.3 V vs. Li^+/Li. After these potentials were hold for 45 h, the cells were discharged, the aluminum current collector was carefully removed. Accordingly, XP spectra were collected at the surface oriented towards the aluminum current collector. In Figure 6 the peaks at 532.7 eV and 528.7 eV in the O 1s spectra can be assigned to the C–O bonds of PEO[18] and the lattice oxygen in NCM,[45] according to literature. While no changes in the O 1s spectra of the OCV and 4.1 V cell can be seen, a new signal at 531.1 eV, corresponding to the C=O group, is detected in the spectrum of the 4.3 V cell. This is in good agreement with previous XPS investigations.[46,47] In addition, in the C 1s spectra the peaks at 286.6 eV and 284.8 eV can be assigned to C–O and C–C/C–H bonds, respectively. In agreement with the O 1s spectra, the formation of the C=O bond at 288.4 eV is seen in the C 1s spectra of the 4.3 V cell.

Overall, these data show that there is indeed oxidative degradation of PEO at the interface to the active material that cannot be detected by FTIR. This means that the interfacial instability at the cathode side needs to be considered, and we believe that these oxidative degradation products might indeed lead to fast capacity fading in PEO-based SSBs with high voltage cathodes (Figure 3).

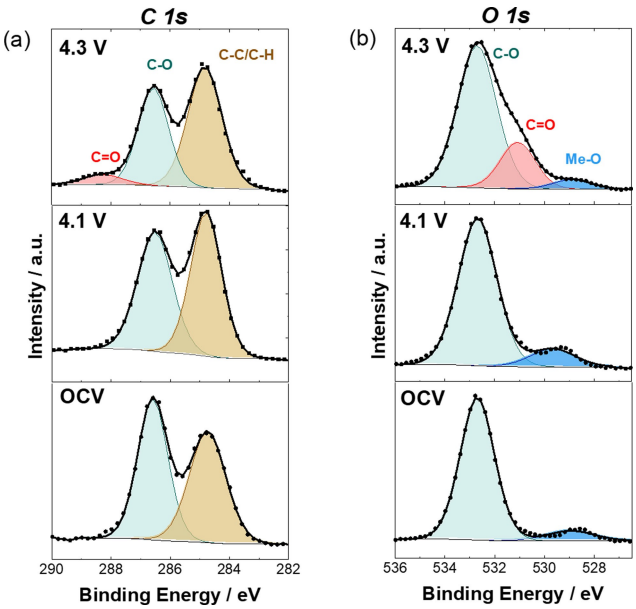

Figure 6. Post-mortem XPS analysis of the SPE/NCM interface using PEO with $M_w = 8\,000\,000\ g\,mol^{-1}$. (a) C 1s spectra and (b) O 1s spectra are shown. The cells were hold at OCV, at 4.1 V or 4.3 V vs. Li^+/Li for 45 h. Surface oriented towards the aluminum current collector was examined with XPS.

Nevertheless, the results obtained to this point suggest that the failure of the SPE cell is an interplay of dendrite growth on the anode side and additional oxidative degradation on the cathode side. However, the effects of oxidative degradation at the interface with the cathode active material do not appear to be as severe as previously reported in the literature. Still, further studies on the PEO/NCM interface for a deeper understanding are needed.

Conclusion

In this study, the compatibility of PEO-based SSBs in combination with high-voltage cathodes is critically evaluated and improved. The hypothesis of the formation of lithium dendrites associated with the failure of high-voltage cells, indicated by "voltage noise" behavior during galvanostatic charging, is confirmed by detection of reaction products of lithium dendrites with LATP. To overcome this failure, an SPE with a higher molecular weight PEO was used, which improved the mechanical rigidity of the SPE and enabled reasonable cycling performance with NCM compared to low molecular weight PEO. Furthermore, we show that often overlooked effects, such as cell leakage and elevated temperatures during cycling, can easily lead to incorrect conclusions about the oxidative degradation of the PEO, when FTIR is used as an analytical technique. Using a more surface sensitive technique like XPS, we demonstrate the formation of oxidative degradation products at the SPE/NCM interface unequivocally. The detailed investigation of this interface degradation and its influence on cell performance, depending on the specific cathode active material and cell voltage will be elucidated in further studies.

Acknowledgements

The authors would like to acknowledge the financial support from the Federal Ministry of Education and Research (BMBF) within the FestBatt II project (03XP0433D and 03XP0429B). D.B. and S.P. would like to thank moreover the Helmholtz Association for the basic funding. A.H. would like to thank the "Professorinnenprogramm III" funded by BMBF. Open Access funding enabled and organized by Projekt DEAL.

Conflict of Interest

The authors declare no conflict of interest.

Data Availability Statement

The data that support the findings of this study are available from the corresponding author upon reasonable request.

Keywords: Cell Failure · High Voltage Cathodes · Interface Stability · Poly(ethylene Oxide) · Solid-State Batteries

[1] J. Janek, W. G. Zeier, *Nat. Energy* **2016**, *1*, 16141.
[2] Y. Kato, S. Hori, T. Saito, K. Suzuki, M. Hirayama, A. Mitsui, M. Yonemura, H. Iba, R. Kanno, *Nat. Energy* **2016**, *1*, 16030.
[3] G. E. Blomgren, *J. Electrochem. Soc.* **2017**, *164*, A5019–A5025.
[4] T. Krauskopf, F. H. Richter, W. G. Zeier, J. Janek, *Chem. Rev.* **2020**, *120*, 7745.
[5] P. Yao, H. Yu, Z. Ding, Y. Liu, J. Lu, M. Lavorgna, J. Wu, X. Liu, *Front. Chem.* **2019**, *7*, 522.
[6] A. Kim, S. Woo, M. Kang, H. Park, B. Kang, *Front. Chem.* **2020**, *8*, 468.
[7] D. Park, H. Park, Y. Lee, S.-O. Kim, H.-G. Jung, K. Yoon Chung, J. Hyung Shim, S. Yu, *ACS Appl. Mater. Interfaces* **2020**, *12*, 34806.
[8] S. S. Berbano, M. Mirsaneh, M. T. Lanagan, C. A. Randall, *Int. J. Appl. Glass Sci.* **2013**, *4*, 414.
[9] A. Varzi, R. Raccichini, S. Passerini, B. Scrosati, *J. Mater. Chem. A* **2016**, *4*, 17251.
[10] J. Qiu, X. Liu, R. Chen, Q. Li, Y. Wang, P. Chen, L. Gan, S. -J Lee, D. Nordlund, Y. Liu, X. Yu, X. Bai, H. Li, L. Chen, *Adv. Funct. Mater.* **2020**, *30*, 1909392.
[11] R. Chen, Q. Li, X. Yu, L. Chen, H. Li, *Chem. Rev.* **2020**, *120*, 6820.
[12] Z. Xue, D. He, X. Xie, *J. Mater. Chem. A* **2015**, *3*, 19218.
[13] J. Ravi Nair, L. Imholt, G. Brunklaus, M. Winter, *Electrochem. Soc. Interface* **2019**, *28*, 55.
[14] A. Maurel, M. Armand, S. Grugeon, B. Fleutot, C. Davoisne, H. Tortajada, M. Courty, S. Panier, L. Dupont, *J. Electrochem. Soc.* **2020**, *167*, 070536.
[15] T. Kobayashi, Y. Kobayashi, M. Tabuchi, K. Shono, Y. Ohno, Y. Mita, H. Miyashiro, *ACS Appl. Mater. Interfaces* **2013**, *5*, 12387.

[16] J. Liang, Y. Sun, Y. Zhao, Q. Sun, J. Luo, F. Zhao, X. Lin, X. Li, R. Li, L. Zhang, S. Lu, H. Huang, X. Sun, *J. Mater. Chem. A* **2020**, *8*, 2769.
[17] Z. Chen, G.-T. Kim, Z. Wang, D. Bresser, B. Qin, D. Geiger, U. Kaiser, X. Wang, Z. Xiang Shen, S. Passerini, *Nano Energy* **2019**, *64*, 103986.
[18] L. Seidl, R. Grissa, L. Zhang, S. Trabesinger, C. Battaglia, *Adv. Mater. Interfaces* **2022**, *9*, 2100704.
[19] Y. Xia, T. Fujieda, K. Tatsumi, P. Paolo Prosini, T. Sakai, *J. Power Sources* **2001**, *92*, 234.
[20] K. Nie, X. Wang, J. Qiu, Y. Wang, Q. Yang, J. Xu, X. Yu, H. Li, X. Huang, L. Chen, *ACS Energy Lett.* **2020**, *5*, 826.
[21] G. Homann, L. Stolz, J. Nair, I. Cekic Laskovic, M. Winter, J. Kasnatscheew, *Sci. Rep.* **2020**, *10*, 4390.
[22] G. Hernández, I. L. Johansson, A. Mathew, C. Sångeland, D. Brandell, J. Mindemark, *J. Electrochem. Soc.* **2021**, *168*, 100523.
[23] E. Simonetti, M. Carewska, M. Di Carli, M. Moreno, M. de Francesco, G. B. Appetecchi, *Electrochim. Acta* **2017**, *235*, 323.
[24] G. Homann, L. Stolz, K. Neuhaus, M. Winter, J. Kasnatscheew, *Adv. Funct. Mater.* **2020**, *30*, 2006289.
[25] C. Wang, T. Wang, L. Wang, Z. Hu, Z. Cui, J. Li, S. Dong, X. Zhou, G. Cui, *Adv. Sci.* **2019**, *6*, 1901036.
[26] K. Matsumoto, K. Inoue, K. Nakahara, R. Yuge, T. Noguchi, K. Utsugi, *J. Power Sources* **2013**, *231*, 234.
[27] M. Nakayama, S. Wada, S. Kuroki, M. Nogami, *Energy Environ. Sci.* **2010**, *3*, 1995.
[28] H.-K. Tian, R. Jalem, B. Gao, Y. Yamamoto, S. Muto, M. Sakakura, Y. Iriyama, Y. Tateyama, *ACS Appl. Mater. Interfaces* **2020**, *12*, 54752.
[29] Y. Zhu, X. He, Y. Mo, *ACS Appl. Mater. Interfaces* **2015**, *7*, 23685.
[30] Q. Cheng, A. Li, N. Li, S. Li, A. Zangiabadi, T.-D. Li, W. Huang, A. Ceng Li, T. Jin, Q. Song, W. Xu, N. Ni, H. Zhai, M. Dontigny, K. Zaghib, X. Chuan, D. Su, K. Yan, Y. Yang, *Joule* **2019**, *3*, 1510.
[31] A. Gupta, E. Kazyak, N. Craig, J. Christensen, N. P. Dasgupta, J. Sakamoto, *J. Electrochem. Soc.* **2018**, *165*, A2801–A2806.
[32] L. Stolz, G. Homann, M. Winter, J. Kasnatscheew, *Mater. Adv.* **2021**, *2*, 3251.
[33] C. Wang, Y. Yang, X. Liu, H. Zhong, H. Xu, Z. Xu, H. Shao, F. Ding, *ACS Appl. Mater. Interfaces* **2017**, *9*, 13694.
[34] D. Devaux, R. Bouchet, D. Glé, R. Denoyel, *Solid State Ionics* **2012**, *227*, 119.
[35] M. H. Cho, J. Trottier, C. Gagnon, P. Hovington, D. Clément, A. Vijh, C.-S. Kim, A. Guerfi, R. Black, L. Nazar, K. Zaghib, *J. Power Sources* **2014**, *268*, 565.
[36] L. Wang, B. Chen, J. Ma, G. Cui, L. Chen, *Chem. Soc. Rev.* **2018**, *47*, 6505.
[37] S. Song, X. Peng, K. Huang, H. Zhang, F. Wu, Y. Xiang, X. Zhang, *Nanoscale Res. Lett.* **2020**, *15*, 110.
[38] J. Ma, Z. Liu, B. Chen, L. Wang, L. Yue, H. Liu, J. Zhang, Z. Liu, G. Cui, *J. Electrochem. Soc.* **2017**, *164*, A3454–A3461.
[39] D. J. Lyman, R. Benck, S. Dell, S. Merle, J. Murray-Wijelath, *J. Agric. Food Chem.* **2003**, *51*, 3268.
[40] L. H. Sim, S. N. Gan, C. H. Chan, R. Yahya, *Spectrochim. Acta Part A* **2010**, *76*, 287.
[41] K. K. Kumar, M. Ravi, Y. Pavani, S. Bhavani, A. K. Sharma, V. V. R. N. Rao, *J. Non-Cryst. Solids* **2012**, *358*, 3205.
[42] H. T. Ahmed, O. Gh Abdullah, *Polymers* **2019**, *11*, 853.
[43] M. A. K. L. Dissanayake, R. Frech, *Macromolecules* **1995**, *28*, 5312.
[44] L.-L. I. Fockaert, D. Ganzinga-Jurg, J. Versluis, B. Boelen, H. J. Bakker, H. Terryn, J. M. C. Mol, *J. Phys. Chem. C* **2020**, *124*, 7127.
[45] R. Li, Y. Ming, W. Xiang, C. Xu, G. Feng, Y. Li, Y. Chen, Z. Wu, B. Zhong, X. Guo, *RSC Adv.* **2019**, *9*, 36849.
[46] J. Li, Y. Ji, H. Song, S. Chen, S. Ding, B. Zhang, L. Yang, Y. Song, F. Pan, *Nano-Micro Lett.* **2022**, *14*, 191.
[47] J. Liang, D. Chen, K. Adair, Q. Sun, N. Graham Holmes, Y. Zhao, Y. Sun, J. Luo, R. Li, L. Zhang, S. Zhao, S. Lu, H. Huang, X. Zhang, C. Veer Singh, X. Sun, *Adv. Energy Mater.* **2021**, *11*, 2002455.

Manuscript received: December 13, 2022
Accepted manuscript online: January 10, 2023
Version of record online: February 10, 2023